Order and Dynamics of a Series of Side Chain Liquid Crystal Copolymers through ^{2}H NMR Spectroscopy

Evgueni Barmatov

Chemistry Department, Moscow State University, 119899 Moscow, Russia

Leonardo Chiezzi, Silvia Pizzanelli, and Carlo Alberto Veracini*

Dipartimento di Chimica e Chimica Industriale, Università degli Studi di Pisa, via Risorgimento 35, 56126 Pisa, Italy

Received November 2, 2001

ABSTRACT: The order and dynamics of the mesogenic groups in a series of side chain liquid crystal copolymers were investigated in their nematic phase through ^{2}H NMR. The main chain is built with a variable content of randomly distributed acrylic and methacrylic units, while the mesogenic groups are based on a phenyl benzoate moiety which is labeled on one phenyl ring. The analysis of the orientational order together with the spectral densities $J_1(\omega_0)$ and $J_2(2\omega_0)$ revealed a certain degree of heterogeneity concerning both the order of the mesogens *a* and *m* respectively bound to the acrylic and the methacrylic monomers and their dynamics. In fact, mesogens *m* are more ordered than *a* and characterized by slower motions. The processes mainly contributing to relaxation proved to be the rotation of the phenyl ring about its para-axis and the spinning of the whole mesogenic unit.

1. Introduction

^{2}H NMR studies of the order and dynamics of some side chain liquid crystalline polyacrylates and polymethacrylates have been reported.[1] In particular, the determination of the order of the various parts constituting the system, that is, the side chain mesogens, the spacer, and the main chain, allowed a certain degree of coupling among these parts to be revealed. In addition, an opposite tendency in the relative arrangement of the side chain and the backbone was found in polyacrylates and polymethacrylates, the mesogenic side groups tending to be respectively parallel and perpendicular to the main chain. In this paper the order of the side chains in systems whose backbone is made of both acrylic and methacrylic units is investigated with the aim of finding out if the skeleton composition affects the order of the side chains and, in particular, if different degrees of side chain order are found in a given copolymer.

As far as the side chain dynamics is concerned, the studies previously mentioned mainly dealt with the motions in the glassy state. It has been observed that the motions in the mesophase region approaching the glass transition are characterized by frequencies comparable with the quadrupolar interaction. Furthermore, dielectric spectroscopy has been employed to study the dynamics of polyacrylates and polymethacrylates in the frequency range from 10^{-2} to 10^6 Hz[2], and several relaxation processes have been observed and assigned to different parts of the system. In particular, besides γ-relaxation processes assigned to reorientations of the tail and the spacer groups and an α-relaxation connected with the segmental motions of chain backbone, a β- and a δ-relaxation were assigned to the rotational fluctuation of the mesogenic group around its long and short axis, respectively. However, the β-process was observed only in the glass region as in the region of stability of the mesophase it is sensitive to frequencies higher than the maximum investigated, while δ-process was characterized by a maximum frequency of about 10^4 Hz. Here we intend to investigate the motion related to the β-process in the range of stability of the mesophase, our technique being sensitive to frequencies higher than 10^6 Hz. Other faster dynamic processes, such as the motions of a fragment belonging to the mesogenic unit, will possibly contribute to the relaxation processes tested by us, whereas we will not be able to give insight into the too slow rotation around the short molecular axis.

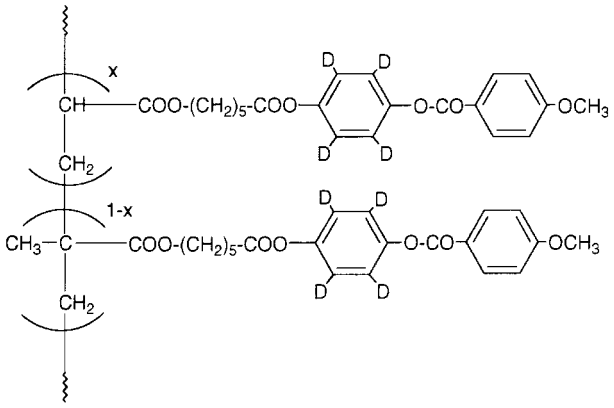

Figure 1. Series of polymers under study. **P30**: g 40 °C N 114 °C I; **P50**: g 26 °C N 112 °C I; **P70**: g 26 °C N 118 °C I; **P85**: g 24 °C N 120 °C I.

2. Experimental Section

The structure and phase behavior of the ^{2}H-labeled side chain liquid crystal polymers are shown in Figure 1. The polymers differ in the composition, the acrylic molar fraction *x* being 0.30, 0.50, 0.70, and 0.85 for the different samples. The name used to refer to a given polymer characterized by the molar fraction *x* is P*x*·100.

The copolymers were obtained by radical copolymerization of the selectively deuterated monomers 4-methoxybenzoic acid

* Corresponding author: Fax +39-050-918-260; e-mail verax@dcci.unipi.it.

10.1021/ma011913w CCC: $22.00
Published on Web 03/09/2002

Table 1. Molecular Weight Characteristics of the Copolymers under Examination

sample	M_w	M_w/M_n
P30	32 000	1.8
P50	28 000	1.6
P70	32 000	1.8
P85	27 000	1.6

4-[6-(2-methylacryloyloxy)hexanoyloxy]phenyl-d_4 ester (**M1**) and 4-methoxybenzoic acid 4-(6-acryloyloxyhexanoyloxy)phenyl-d_4 ester (**M2**) in absolute toluene at 70 °C. AIBN (2 wt %) was used as initiating agent. They were purified by repeated reprecipitation from toluene solutions by ethanol. The monomers were synthesized according to an earlier described procedure.[3] According to ^{1}H NMR spectroscopy, the degree of deuteriation of **M1** and **M2** was 98.0 ± 0.2%. (^{1}H NMR spectra were recorded on a Bruker 300 MSL spectrometer operating at 299.96 MHz.)

M1: ^{1}H NMR ($CDCl_3$): δ (ppm) 8.12 (d, 2H, Ph); 7.19 (d, 2H*, Ph); 7.10 (d, 2H*, Ph); 6.95 (d, 2H, Ph); 6.1 (d, 1H, trans CH_2═C); 5.55 (d, 1H, cis CH_2═C); 4.15 (t, 2H, COO−CH_2); 3.81 (s, 3H, OCH_3); 2.61 (t, 2H, CH_2−COO); 1.95 (s, 3H, CH_3); 1.5−1.9 (m, 6H, CH_2).

M2: ^{1}H NMR ($CDCl_3$): δ (ppm) 8.12 (d, 2H, Ph); 7.20 (d, 2H*, Ph); 7.11 (d, 2H*, Ph); 6.95 (d, 2H, Ph); 6.35 (dd, 1H, CH_2═CH); 6.12 (dd, 1H, CH_2═C*H*); 5.81 (dd, 1H, CH_2═CH); 4.15 (t, 2H, COO−CH_2); 3.98 (s, 3H, −CH_3); 2.55 (t, 2H, −CH_2−COO); 1.4−1.9 (m, 6H, −CH_2−).

The symbol * indicates the low-intensity residual signals.

Molecular weights and dispersity ratios of the copolymers were determined by gel permeation chromatography using a Waters 2690 instrument equipped with a set of PL columns and a refraction index detector Waters 2410. THF was used as a solvent (1 mL min^{-1}, 25 °C) and a calibration plot constructed with polystyrene standards. The molecular weight characteristics of the copolymers are given in Table 1.

The composition of each copolymer was assumed to be equal to the feed composition in the reaction of polymerization, as this reaction was conducted to a quantitative conversion. The phase behavior of the copolymers was studied by polarized optical microscopy, DSC, and X-ray. Optical microscopy observations were made with a Zeiss polarizing microscope equipped with a Mettler FP-82HT hot stage controlled by a Mettler FP90 unit. Phase transitions were studied by differential scanning calorimetry (DSC 2010, TA Instruments) at a scanning rate of 10 °C min^{-1} from −10 to 250 °C in nitrogen. The DSC cell was calibrated with indium. X-ray diffraction analysis was carried out using an URS-55 instrument (Ni-filtered Cu Kα radiation).

^{2}H NMR experiments were performed on a Varian VXR 300 spectrometer operating at 46.04 MHz. A single pulse sequence was used to record a spectrum. The samples, placed in the magnetic field, were heated to the isotropic point and then cooled at a rate of 1 °C/3 min. The $\pi/2$ pulse length was 15 μs, and the number of scans was 512.

A broad-band version of the Jeener−Broekaert pulse sequence[5] was employed for measuring the Zeeman and quadrupolar order decay rates. The numerical computations of correlation functions and corresponding spectral densities were carried out with a modified version of the CAGE software package for Mathematica 4,[6] running on a PC.

3. Theory

3.1. Order Parameter. The quadrupolar coupling of ^{2}H can be related to the molecular axes order parameters S_{zz}, S_{yy}, and S_{xx} according to the following equation

$$\Delta\nu = \frac{3}{2}q\left[S_{zz}\left(\cos^2\theta - \frac{1}{2}\sin^2\theta - \frac{1}{6}\eta\cos^2\theta + \frac{1}{3}\eta\sin^2\theta + \frac{1}{6}\eta\right) + (S_{xx} - S_{yy})\left(\frac{1}{2}\sin^2\theta + \frac{1}{6}\eta\cos^2\theta + \frac{1}{6}\eta\right)\right] \quad (1)$$

where q is the quadrupolar coupling constant, η is the asymmetry parameter, and θ is the angle between the z molecular axis and the z axis of the system where the quadrupolar tensor is diagonal.

This axis lies along the C−D bond direction, and q and η lie within a narrow range for particular kinds of bonds.[7]

3.2. Dynamics. The interpretation of the spectral densities $J_1(\omega_0)$ and $J_2(2\omega_0)$ has been carried out by means of several available motional models, which are briefly reviewed in the following.

In liquid crystal polymers, dynamics can be treated in terms of models originally developed for low molecular weight liquid crystals. Different dynamic processes have been identified and assumed to be independent especially on the basis of time scale arguments. The processes are usually classified as intramolecular, "overall molecule", and collective, in order of increasing time scales.[8]

For the system in question, the intramolecular motion consists of the rotation of the phenyl ring about its para-axis. Different models for the motion about a single axis have been used, in particular (i) isotropic strong collisions,[9] (ii) small steps rotational diffusion,[9,10] and (iii) rotation hindered by barriers of 2-fold symmetry.[11] The first model allows jumps between sites equally spaced about the rotational axis with equal jump probabilities from any site to any other. If the jumps are restricted to occur only among nearest neighbors and in the limit of an infinite number of sites, the model is known as small step rotational diffusion (ii). Model iii treats the motion as a process occurring in a 2-fold symmetric potential depending on the rotational angle ϕ, $V(\phi) = V_0[(1 - \cos 2\phi)/2]^\rho$ where the flip across the energy maxima and the motion within the potential minima (libration) are considered as coupled processes.

The "overall molecule" (here meant to be the mesogenic unit in the side chain) dynamics has been assumed decoupled from the polymer chain motion on the basis of time scale considerations. In systems similar to the ones under study the backbone has been found to be motionally characterized by correlation times of the order of tens of milliseconds at 10−30 K above the glass transition,[1e] and frequencies up to about 10^4 Hz were reported for a similar polymethacrylate studied in the whole mesophase temperature region.[2c] Side chains motions sensitive to our experimental data are at least more than 2 orders of magnitude faster than the main chain motion, as it will be shown in the following. Therefore, the main chain provides a static environment to the mesogens and can be considered still with respect to them. The model we adopted here is generally referred as Nordio model,[12] where the spinning around the long molecular axis and the tumbling of this axis are taken into account.

The collective dynamics is of little importance in high field spin relaxation which is sensitive to motions with characteristic frequencies much higher than the ones involved in collective dynamic processes.[13] In addition, since the angle between the aromatic C−D bond and the magnetic field is close to the magic angle, the contribution of fluctuations of order director to spectral densities can be safely neglected.[14,15]

The relaxation times for Zeeman (T_{1Z}) and quadrupolar order (T_{1Q}) in a system of uncoupled deuterons

are related to spectral densities $J_M(M\omega_0)$ by the following equations:

$$1/T_{1Z} = J_1(\omega_0) + 4J_2(2\omega_0)$$
$$1/T_{1Q} = 3J_1(\omega_0) \quad (2)$$

where the spectral densities are defined as one-sided Fourier transforms of the correlation functions $G_M(t)$:

$$J_M(\omega) = \int_0^\infty \mathrm{d}t\, G_M(t)\mathrm{e}^{-i\omega t}, \quad M = 1, 2 \quad (3)$$

If internal motions are assumed uncorrelated to "overall molecule" motions, the correlation function $G_M(t)$ can be written as a product of individual correlation functions

$$G_M(t) = C\sum_{KK'}\sum_{NN'} C^{(\mathrm{mol})}_{MKK'} U_{KK'NN'} C^{(\mathrm{int})}_{NN'}(t) \quad (4)$$

where $C = (3/8)(e^2qQ/\hbar)^2$ and $U_{KK'NN'}$ transforms the phenyl ring based frame into the laboratory system.

Within Nordio model, the spinning and tumbling of the long molecular axis are described by the coefficients $D_{\|}$ and $D_{\perp}$, respectively. They appear in the "overall molecule" correlation function $C^{(\mathrm{mol})}_{MKK'}(t)$ according to the following equation

$$C^{(\mathrm{mol})}_{MKK'}(t) = \delta_{KK'} c_{MK} \sum_{i=0}^{\infty} a^{(i)}_{MK} \exp(-\lambda^{(i)}_{MK} t)$$

where

$$\lambda^{(i)}_{MK} = \frac{6D_{\perp}}{b^{(i)}_{MK}} + K^2(D_{\|} - D_{\perp}) \quad (5)$$

and $a^{(i)}_{MK}$, $b^{(i)}_{MK}$, and c_{MK} have been calculated in ref 16 as a function of the principal order parameter for a Maier–Saupe potential.

The correlation function $C^{(\mathrm{int})}_{NN'}(t)$ describes the rotation about the para-axis of the phenyl ring. In the isotropic strong collision (i) and in the small step rotational diffusion (ii) models it has the following form:

$$C^{(\mathrm{int})}_{NN'}(t) = \delta_{NN'} \exp[-k_N t] \quad (6)$$

where $k_0 = 0$, $k_1 = D_\phi$, and $k_2 = (3\nu + 1)k_1$, being $\nu = 0$ for (i)[9,17] and $\nu = 1$ for (ii).[9,10,18]

Within model iii[19] it can be written as

$$C^{(\mathrm{int})}_{NN'}(t) = \sum_{j=0}^{\infty} b^{(j)}_{NN'} \exp(-\xi^{(j)}_{NN'} D_\phi t) \quad (7)$$

where $b^{(j)}_{NN'}$ and $\xi^{(j)}_{NN'}$ have been calculated with the procedure described by Edholm and Blomberg.[11]

The form of the potential allows an independent variation of the potential shape through ρ and of the barrier maxima V_0. When V_0 is equal to zero, the model turns to model ii. Increasing the value of ρ has the effect of broadening the potential wells and leads to increased librational amplitudes.

4. Results and Discussion

4.1. Order. The ^{2}H spectrum of all the samples consists of a sole quadrupolar doublet, whose peaks are characterized by a line width ranging from around 1000 to 4000 Hz. The systems might be expected to show more than one doublet because both different deuterium nuclei are present and labeled side chains are bound to different monomers, this possibly resulting in different degrees of side chain order.

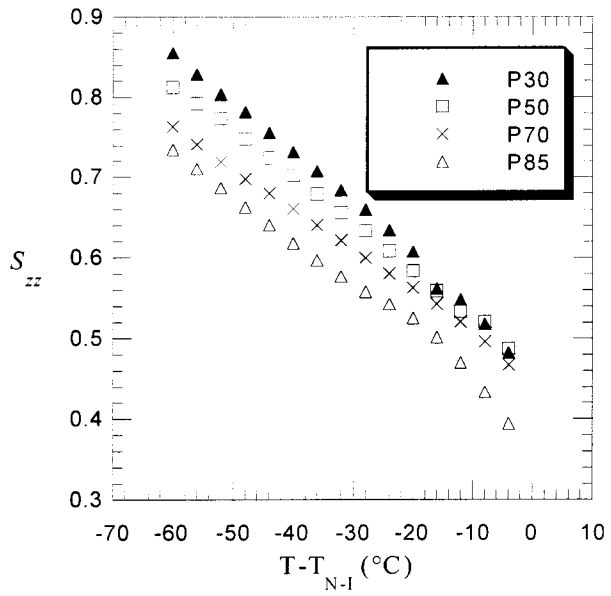

Figure 2. Temperature dependence of the order parameter S_{zz} for the series of polymers under study. Polymers **P30**, **P50**, **P70**, and **P85** are represented by filled triangles, squares, crosses, and open triangles, respectively. T_{N-I} is the transition temperature between the nematic and isotropic phase.

In fact, deuteria 2 and 6, as well as 3 and 5, are made equivalent by the rotation of the phenyl moiety, and the adjacent deuteria 2, 3 (or 5, 6), despite their possible small inequivalency, cannot be distinguished because of the broad line width.

On the other hand, the evidence of a sole quadrupolar doublet rules out the presence of remarkably different degrees of side chain order in every system examined, although more modest heterogeneities are compatible with the spectra within a 5% indetermination on the order parameters.

The order parameter S_{zz} of the aromatic core of the mesogenic side groups has been evaluated from the ^{2}H spectra. The experimental quadrupolar splitting is related to S_{zz} through eq 1. The constants q, η, and θ have been set to 185 kHz,[7] 0.04,[7] and 60°, respectively. The biaxiality $S_{xx}-S_{yy}$ has been assumed to be 0.04 on the basis of values reported for similar compounds.[20]

Figure 2 shows S_{zz} as a function of the temperature $T - T_{N-I}$ for the polymers in question. S_{zz} is dependent on the polymer composition, being higher when the acrylic molar fraction is lower.

This evidence is consistent with the two following hypotheses: (a) the increase of acrylic content in the backbone determines a lower degree of order for all the mesogenic units, and (b) side chains bound to acrylic monomers are less ordered than side chains bound to methacrylic ones, the different degrees of order being actually covered by the broad line width of the peaks.

In addition, S_{zz} is found to change linearly with the composition at a given temperature, as pictured in Figure 3 as an example. This evidence does not allow to rule out any of previous hypotheses.

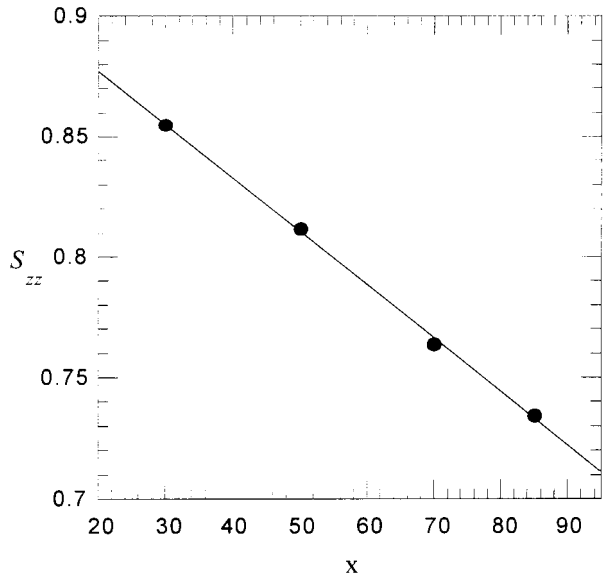

Figure 3. S_{zz} dependence on the acrylic molar fraction x at the temperature $T - T_{N-I} = -60$ °C.

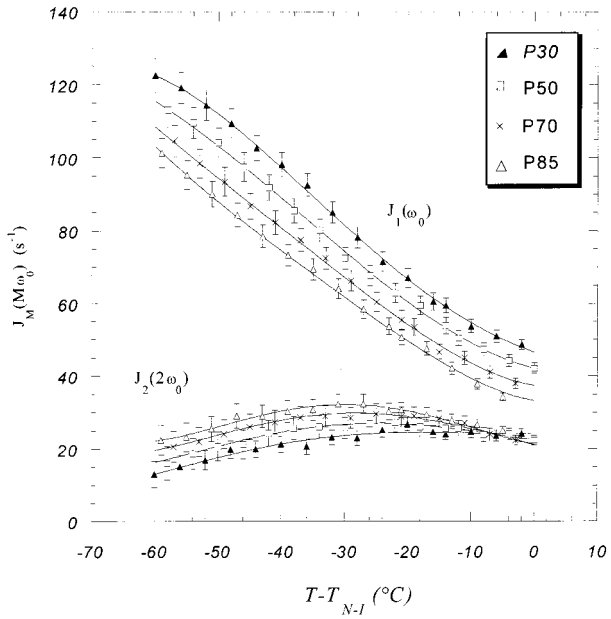

Figure 4. Temperature trends of the experimental (symbols) and calculated (solid lines) spectral densities $J_1(\omega_0)$ and $J_2(2\omega_0)$ of the copolymers. The spectral densities were obtained using eq 10, where $J_{Ma}(M\omega_0,T-T_{N-I})$ and $J_{Mm}(M\omega_0,T-T_{N-I})$ assume the values calculated with the best-fitting parameters of Table 2.

The analysis of the spectral densities developed in the following paragraph will show that the hypothesis b is consistent with the whole data set.

4.2. Dynamics. The spectral densities $J_1(\omega_0)$ and $J_2(2\omega_0)$ show similar trends vs temperature for the polymers examined (see Figure 4). $J_1(\omega_0)$ decreases with $T - T_{N-I}$ from a maximum at low temperature while $J_2(2\omega_0)$ tends to increase in most of the temperature range examined, reaching a maximum which is shifted at higher temperatures when the acrylic content is decreased.

The slight differences observed in the series indicate that the dynamics of the mesogenic units in the side chain is affected by the composition of the backbone.

The experimental spectral densities have been fitted using a global target approach; i.e., the data have been simultaneously fitted over a range of temperatures, assuming a given form for the temperature dependence of the diffusional coefficients. The fitting routine minimizes the quantity

$$E = \sum_i \sum_M \left[\frac{J_M^{(\mathrm{calc})}(M\omega_0,i) - J_M^{(\mathrm{exp})}(M\omega_0,i)}{J_M^{(\mathrm{exp})}(M\omega_0,i)} \right]^2 \qquad (8)$$

where $J_M^{(\mathrm{calc})}(M\omega_0,i)$ and $J_M^{(\mathrm{exp})}(M\omega_0,i)$ are the calculated and experimental spectral densities at the ith temperature and $M = 1, 2$.

The diffusional coefficients for "overall molecule" motions ($D_{\|}$ and $D_{\perp}$) and for internal motion (D_ϕ) have been assumed to have an Arrhenius temperature dependence:

$$D_k = D_k^{\infty} \mathrm{e}^{-E_a^k/RT} \qquad (9)$$

with $D_k = D_{\|}$, $D_{\perp}$, and D_ϕ.

To find out the nature of the motions actually involved, at first we applied simulation procedures which could at least reproduce the temperatures where the spectral densities show the maxima and the experimental trend.

As a first step, we just considered the internal motion and applied (i), (ii), and (iii) models. Within model ii, $J_1(\omega_0)$ trend showed a maximum at higher temperature than $J_2(2\omega_0)$ maximum, which is opposite to the experimental behavior. Model i provided spectral density curves able to reproduce the relative positions of the temperatures corresponding to the maxima, i.e., $J_1(\omega_0)$ showing a maximum at a lower temperature and $J_2(2\omega_0)$ at a higher one. However, the experimental positions of these temperatures were matched by the calculated ones only when the activation energy characterizing the motion in question was set at about 10 kJ mol^{-1}, which imposed, on the other hand, that the calculated spectral densities were remarkably higher than the experimental values.

For the spectral densities calculated through model iii with values of $V_0 + E_\phi < 15$ kJ mol^{-1}, the positions of the temperatures corresponding to the maxima were well reproduced. As far as the trend is concerned, the $J_1(\omega_0)$ trend was reasonably described in all the temperature range investigated, but the model failed in reproducing $J_2(2\omega_0)$, whose experimental trend is remarkably sloped at low temperatures whereas the curve calculated was rather flat. On the other hand, the $J_2(2\omega_0)$ trend could be reproduced only when higher values of $V_0 + E_\phi$ were imposed, but in this case $J_1(\omega_0)$ was always overestimated. This evidence suggested that two motions are involved: one characterized by a low activation energy and mainly affecting $J_1(\omega_0)$ and the other characterized by a high activation energy and mainly affecting $J_2(2\omega_0)$. On the basis of general considerations concerning hindrance in molecular motions, we hypothesized that the less hindered dynamic process was an internal motion and the more hindered was some "overall molecule" motion.

The addition of an "overall molecule" motion to the internal dynamics described by model iii sensitively improved the calculated spectral densities in the case of the polymer with the highest acrylic content (P85). For the polymer with the lower acrylic content (P30), fitting procedures tended to make the contribution of this motion to spectral densities negligible with respect

to the internal one. The different role played by the "overall molecule" motion in the polymers characterized by the two extreme backbone compositions considered seemed to be qualitatively acceptable. In fact, if it is assumed that the backbone influence on the dynamics of the side chains results in an increasing mobility in the side chains with increasing acrylic content on the backbone, it seems to be reasonable that for more mobile systems like P85 the "overall molecule" motion characterized by a high activation energy is fast enough to affect spectral densities together with the less hindered internal motion. Correspondingly, when the system is less mobile, as in the case of P30, the "overall molecule" motion is too slow to affect the spectral densities which are now determined just by the internal motion.

However, the experimental data were still not satisfactorily reproduced also after the introduction of the "overall molecule" motion. We hypothesized that the reason for the difficulty in describing the spectral densities was that they were not actually determined by a system characterized by a given mobility related to the main chain composition, but they were instead determined by a system made of two parts (*a* and *m*) with different mobilities. The spectral densities at a given temperature $T - T_{N-I}$ were written as a combination of a portion coming from *a* due to the side chains bound to the acrylic monomers (J_{Ma}) and a portion coming from *m* due to the side chains bound to the methacrylic units (J_{Mm}), each contribution being weighed by the corresponding molar fraction:

$$J_M(M\omega_0,T-T_{N-I}) = xJ_{Ma}(M\omega_0,T-T_{N-I}) + (1-x)J_{Mm}(M\omega_0,T-T_{N-I}) \quad (10)$$

where x is the molar fraction of the acrylic monomers. This equation implies that the contribution to $J_1(\omega_0)$ and $J_2(2\omega_0)$ from each part is not dependent on the polymeric composition and that it has the same value for all the polymers at the same $T - T_{N-I}$.

The experimental data at a given temperature $T - T_{N-I}$ and at the four compositions available were fitted by the equation above, where $J_{Ma}(M\omega_0,T-T_{N-I})$ and $J_{Mm}(M\omega_0,T-T_{N-I})$ are the parameters to be extracted. This procedure provided the $J_{Ma}(M\omega_0)$ and $J_{Mm}(M\omega_0)$ values pictured in Figures 5 and 6. The effectiveness of this data treatment was checked by comparing the experimental spectral densities of each polymer with the spectral densities back-calculated from eq 10 using the best-fitting parameters $J_{Ma}(M\omega_0,T-T_{N-I})$ and $J_{Mm}(M\omega_0,T-T_{N-I})$.

In addition, the values found were checked to be consistent with the experimental Jeener−Broekaert decay curves, described by monoexponential curves at first. The experimental trends were satisfactorily reproduced by a combination of two exponential curves weighed by the composition and whose decay constants were related to $J_{Ma}(M\omega_0,T-T_{N-I})$ and $J_{Mm}(M\omega_0,T-T_{N-I})$ through (2).

The comparison between $J_{Ma}(M\omega_0)$ and $J_{Mm}(M\omega_0)$ trends suggests that the dynamic processes described by $J_{Ma}(M\omega_0)$ are involved also in $J_{Mm}(M\omega_0)$, where they seem to be slowed down with respect to *a*.

Since the order parameter S_{zz} affects the relaxation behavior, the order parameters S_{zza} and S_{zzm} of the side chains *a* and *m*, respectively, were necessary. S_{zz} data were treated analogously to the spectral densities $J_M(M\omega_0)$; that is, S_{zz} values at a given temperature

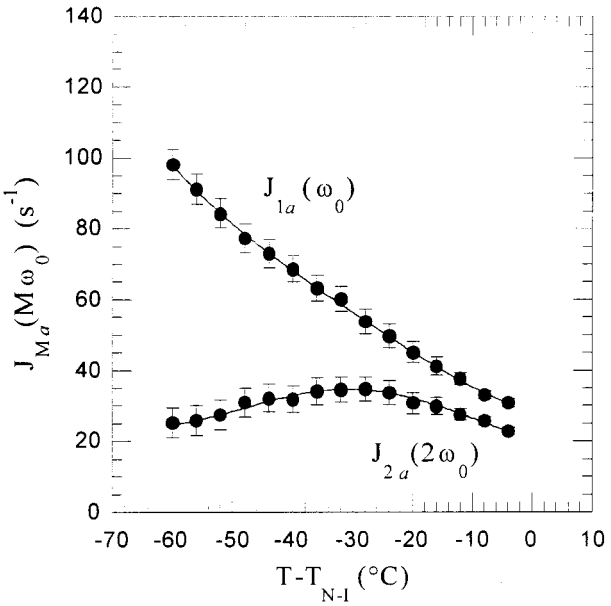

Figure 5. Temperature trends of the spectral densities $J_{1a}(\omega_0)$ and $J_{2a}(2\omega_0)$ extracted from the experimental data according to a procedure outlined in the text (symbols) and the calculated (solid lines) using the best-fitting parameters of Table 2.

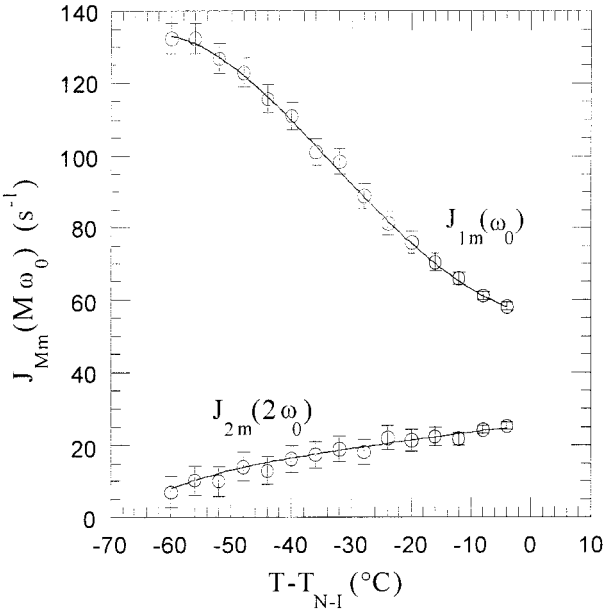

Figure 6. Temperature trends of the spectral densities $J_{1m}(\omega_0)$ and $J_{2m}(2\omega_0)$ extracted from the experimental data according to a procedure outlined in the text (symbols) and the calculated (solid lines) using the best-fitting parameters of Table 2.

$T - T_{N-I}$ and at the four compositions available were fitted by the equation

$$S_{zz}(T-T_{N-I}) = xS_{zza}(T-T_{N-I}) + (1-x)S_{zzm}(T-T_{N-I}) \quad (11)$$

The S_{zza} and S_{zzm} values were checked to be consistent with the experimental spectra. Equation 11 is compatible with the experimental linear dependence of S_{zz} on the composition, pictured in Figure 3 as an example. S_{zzm} is found to be higher than S_{zza} in the whole temperature range, according to the hypothesis (b) outlined in the previous paragraph concerning the order (Figure 7).

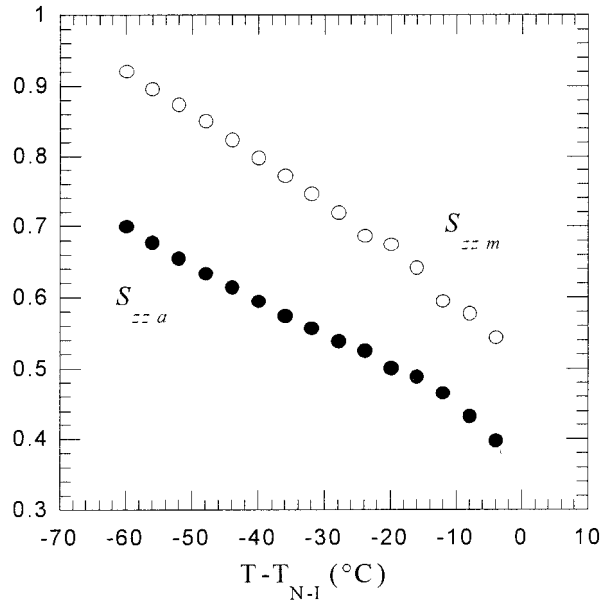

Figure 7. Temperature dependence of the order parameter for the mesogenic side chains bound to the acrylic (S_{zza}) and to the methacrylic (S_{zzm}) monomers.

Table 2. Best-Fitting Parameters for Side Chains Bound to Acrylic (*a*) and to Methacrylic (*m*) Units of the Backbone Obtained by Simultaneously Fitting the Temperature Dependence of $J_{1i}(\omega_0)$ and $J_{2i}(2\omega_0)$, with $i = a, m$

model parameter	*a*	*m*
ρ	12	12
V_0	6 kJ mol^{-1}	6 kJ mol^{-1}
D_{ϕ}^{∞}	3.8×10^{11} s^{-1}	2.5×10^{11} s^{-1}
E_{act}^{ϕ}	13 kJ mol^{-1}	13 kJ mol^{-1}
$D_{\parallel}^{\infty}$	3.0×10^{16} s^{-1}	2.1×10^{15} s^{-1}
$E_{act}^{\parallel}$	58 kJ mol^{-1}	58 kJ mol^{-1}

$J_{Ma}(M\omega_0)$ and $J_{Mm}(M\omega_0)$ data were successfully fitted by a combination of an "overall molecule" motion described by Nordio model and an internal motion described by model iii. The comparison between the values obtained for *a* and *m* (Table 2) agrees with what already suggested by the shape of $J_{Ma}(M\omega_0)$ and $J_{Mm}(M\omega_0)$; that is, the dynamic processes involved in *a* are also present in *m*, where they are found to be slower. In particular, in *m* the "overall molecule" motion is so slowed down that the spectral densities are almost completely described just by the internal motion.

ρ and V_0 were fixed for each fitting, ρ being set to the values 1, 4, 8, 10, 12 and V_0 varied between 0 and 50 kJ mol^{-1}. The quality of the fitting resulted to be quite sensitive to these parameters. For instance, the quantity E defined in eq 8 doubles when ρ is set to 10 and is 10 times higher when V_0 is moved by 1 kJ mol^{-1}.

The values obtained for E_{act}^{ϕ} are comparable in *a* and *m*, and the same has been observed for $E_{act}^{\parallel}$. The error estimated on E_{act}^{ϕ} is about ± 1.5 and ± 1.0 kJ mol^{-1} on $E_{act}^{\parallel}$.

$D_{\perp}^{\infty}$ and $E_{act}^{\perp}$ were included in the fitting parameters at first, but they were ill determined, as already stressed in a recent paper.[6] Therefore, $E_{act}^{\perp}$ was assumed to be the same as $E_{act}^{\parallel}$, and $D_{\perp}^{\infty}$ was fixed to the value inferred from a rough estimated geometry of the mesogenic unit by hydrodynamic arguments for isotropic fluids (5.2×10^{15} s^{-1} in *a* and 3.6×10^{14} s^{-1} in *m*).[21] These values make the contribution of this motion to the spectral densities negligible in all the temperature range. The experimental spectral densities of the polymers, and the ones calculated according to eq 10 using the dynamic parameters of Table 2 are shown in Figure 4.

5. Conclusions

The mesogenic order and dynamics of a series of liquid crystal copolymers deuterated on a phenyl moiety of the side chains have been investigated in their nematic phase by means of ^{2}H NMR. The systems under examination are characterized by the same mesogenic side groups based on phenyl benzoate fragment and differ in the content of the acrylic and methacrylic units in the main chain.

The analysis of the order together with the spectral densities $J_1(\omega_0)$ and $J_2(2\omega_0)$ revealed difference concerning both the order of the mesogens bound to the acrylic (*a*) and the methacrylic (*m*) monomers and their dynamics. We can speculate that this fact might be related to some influence of the monomer of the backbone both on the average orientation of the mesogenic group bound to it and on its dynamics. In other words, the mesogenic side groups prove to be not completely decoupled from the skeleton, according to results already reported for similar compounds where the spacer is built with a number of CH_2 units lower than 6.[22] On the other hand, this difference in *a* and *m*, although consistent with the trend of the experimental order parameter with composition and necessary in the fitting of the spectral densities, is rather surprising as the two fragments *a* and *m* differ just in the presence of a methyl group. In addition, since no heterogeneity is observed by X-rays, optical microscopy, and DSC, it must be extended to a smaller scale than the one detectable by these techniques.

In fact, the groups *m* bound to the methacrylic monomers are slightly more ordered than the side chains *a* bound to the acrylic ones and, moreover, are characterized by a dynamics slower than the others. The processes mainly contributing to relaxation are the rotation of the phenyl ring about its para-axis and the spinning of the whole mesogenic unit in both *a* and *m*.

Furthermore, the relaxation data were found to be very sensitive to the model used to describe the rotation of the phenyl ring about its para-axis. Common models for internal motions in liquid crystals such as isotropic strong collisions and small steps rotational diffusion proved to be inadequate, being necessary to apply a model describing the rotation as a diffusive process in a 2-fold symmetric potential where π flips across the energy maxima and librations are considered as coupled processes. Within this model, librations seem to play an important role, as implied by the high value of the fitting parameter ρ.

References and Notes

(1) (a) Geib, H.; Hisgen, B.; Pschorn, U.; Ringsdorf, H.; Spiess, H. W. *J. Am. Chem. Soc.* **1982**, *104*, 917−919. (b) Boeffel, C.; Hisgen, B.; Pschorn, U.; Ringsdorf, H.; Spiess, H. W. *Isr. J. Chem.* **1983**, *23*, 388−394. (c) Boeffel, C.; Spiess, H. W.; Hisgen, B.; Ringsdorf, H.; Ohm, H.; G.Kirste, R. *Makromol. Chem., Rapid Commun.* **1986**, *7*, 777−783. (d) Boeffel, C.; Spiess, H. W. *Macromolecules* **1988**, *21*, 1626−1631. (e) Germano, G.; Veracini, C. A.; Boeffel, C.; Spiess, H. W. *Mol. Cryst. Liq. Cryst.* **1995**, *266*, 47−58.

(2) (a) Schönhals, A.; Wolff, D.; Springer, J. *Proc. SPIE−Int. Soc. Opt. Eng.* **1996**, *2779*, 424−429. (b) Schönhals, A.; Wolff, D.; Springer, J. *Macromolecules* **1995**, *28*, 6254−6257. (c) Schön-

hals, A.; Gener, U.; Rübner, J. *Macromol. Chem. Phys.* **1995**, *196*, 1671−1685.
(3) Barmatov, E. B.; Yongjie, T.; Kolbina, G. F.; Stennikova, I. N.; Akhmedov, N.; Kozlovskii, M. V.; Shibaev, V. P. *Polym. Sci.* **2001**, *43*, 1−14.
(4) Kobatake, S.; Yamada, B. *Macromol. Chem. Phys.* **1997**, *198*, 2825−2837.
(5) Wimperis, S. *J. Magn. Reson.* **1990**, *86*, 46−59.
(6) Calucci, L.; Geppi, M. *J. Chem. Inf. Comput. Sci.* **2001**, *41*, 1006−1014.
(7) Emsley, J. W. In *Nuclear Magnetic Resonance of Liquid Crystals*; Emsley, J. W., Ed.; Reidel: Dordrecht, 1985; p 379.
(8) Kothe, G.; Stohrer, In *The Molecular Dynamics of Liquid Crystals;* Luckhurst, G. R., Veracini, C. A., Eds.; Kluwer Academic: Dordrecht, 1994; p 195.
(9) Torchia, D. A.; Szabo, A. *J. Magn. Reson.* **1982**, *49*, 107−121.
(10) Wallach, D. *J. Chem. Phys.* **1967**, *47*, 5258−5268.
(11) Edholm, O.; Blomberg, C. *Chem. Phys.* **1979**, *42*, 449−464.
(12) (a) Nordio, P. L.; Busolin, P. *J. Chem. Phys.* **1971**, *55*, 5485−5490. (b) Nordio, P. L.; Rigatti, G.; Segre, U. *J. Chem. Phys.* **1972**, *56*, 2117−2123.
(13) Zeuner, U.; Dippel, T.; Noack, F.; Müller, K.; Mayer, C.; Heaton, N.; Kothe, G. *J. Chem. Phys.* **1992**, *97*, 3794−3802.
(14) Pincus, P. *Solid State Commun.* **1969**, *7*, 415−418.
(15) Blinc, R.; Hogenboom, D.; O'Reilly, D.; Peterson, E. *Phys. Rev. Lett.* **1969**, *23*, 969−972.
(16) Vold, R. R.; Vold, R. L. *J. Chem. Phys.* **1988**, *88*, 1443−1457.
(17) Beckmann, P. A.; Emsley, J. W.; Luckhurst, G. R.; Turner, D. L. *Mol. Phys.* **1986**, *59*, 97−125.
(18) Dong, R. Y. *Mol. Cryst. Liq. Cryst.* **1986**, *141*, 349−359.
(19) Heaton, N. J.; Kothe, G. *J. Chem. Phys.* **1998**, *108*, 8199−8213.
(20) (a) Emsley, J. W.; Furby, M. I. C.; De Luca, G. *Liq. Cryst.* **1996**, *21*, 877−883. (b) Catalano, D.; Cavazza, M.; Chiezzi, L.; Geppi, M.; Veracini, C. A. *Liq. Cryst.* **2000**, *27*, 621−627.
(21) Perrin, F. *J. Phys. Radium* **1934**, *5*, 497−511.
(22) (a) Finkelmann, H.; Ringsdorf, H.; Wendorff, J. H. *Makromol. Chem.* **1978**, *179*, 273−276. (b) Finkelmann, H.; Happ, M.; Portugall, M.; Ringsdorf, H. *Makromol. Chem.* **1978**, *179*, 2541−2544.

MA011913W